P149

Designing a detection scan for adaptive weather sensing

David A. Warde,* Igor Ivic, and Eddie Forren
Cooperative Institute for Mesoscale Meteorological Studies, The University of Oklahoma, and
NOAA/OAR National Severe Storms Laboratory, Norman, Oklahoma

1. INTRODUCTION

Fast adaptive weather scanning was first demonstrated on the National Weather Radar Testbed (NWRT) Phased Array Radar (PAR) in 2009 with the implementation of the Adaptive Digital Signal Processing Algorithm for Phased-Array Radar Timely Scans (ADAPTS) (Heinselman et al. 2009, Priegnitz 2009, and Torres et al. 2009). The algorithm effectively addresses the interest of meteorologists for faster updates by providing spatially focused weather observations to reduce volumetric scanning times and increase overall dwell times in regions of interest.

Initially, in ADAPTS I, beams of a predefined volume coverage pattern (VCP) were turned "on" and "off" based on weather detections and the spatial proximity to those weather detections. The beams that are turned "on" by ADAPTS are referred to as weather beams. At start up and periodically thereafter (to capture developing weather), a complete weather scan (i.e. all beams of the VCP) is performed (see: Heinselman and Torres 2010, Torres et al. 2010).

In ADAPTS II, the need for periodic complete weather scans is eliminated by the introduction of a surveillance scan that is applied in regions where weather beams are "off." Whereas, the weather beam provided sample sizes consistent with good quality estimates as part of the VCP design, the surveillance beam was intentionally limited to only 4 samples for faster volume coverage. To deal with ground clutter contamination, powers removed, by the ground clutter filter, from previous weather beams were fed back into the surveillance processing algorithm. This created a dependency, of the surveillance data processor, on previously scanned weather beams.

ADAPTS III overcomes the dependency on the weather scan and provides flexibility to explore the multifunctional capability needed in the MPAR concept (Heinselman and Torres 2010). This is accomplished by introducing an autonomous detection scan. In this paper, we present the design considerations for a weather detection processing in ADAPTS III that provides fast volume coverage and allows for the use of independent scanning strategies for both weather and detection beams.

* Corresponding Author Address: David A. Warde, CIMMS/University of Oklahoma, National Severe Storms Laboratory, National Weather Center, 120 David L. Boren Blvd. Norman, OK, 73072; David.A.Warde@noaa.gov

2. DETECTION PROCESSING MODE

In ADAPTS III a dedicated mode for scanning a complete volume of space is introduced. Explicitly, the detection scanning strategy includes a 90 degree azimuthal sector (limited by the NWRT PAR single panel design) with observations from surface (0.5 degrees elevation) to 60 degrees in elevation (36 elevations with 54 beams per elevation) in ~7.5 s. The purpose of this mode is timely detection of newly developed weather phenomena. Because this mode is not required to produce operational weather data it was designed to scan a complete volume of space using much shorter dwell times and with coarser azimuthal resolution than weather scans. To save time, the detection mode operates on very few samples (by default 4) per dwell while using pulse repetition times (PRTs) that result in long unambiguous ranges. Additionally, due to clutter contamination constraints (discussed in section 2.2), narrow-spectrum weather with near zero velocity (i.e.: zero-isodop) is significantly attenuated. This is not expected to severely impact the detection performance for two reasons. First, the zero-isodop is not expected to extend radially away from the radar for most weather events except perhaps when laminar flow is predominate. Second and more importantly, the ADAPTS algorithm already provides neighborhood rules that allows for weather growth and advection. The scheduling and use of the detection scan within ADAPTS III as well as ADAPTS evolution is discussed by Priegnitz and Heinselman (2013).

2.1. *Detection Digital Signal Processing Description*

In the first step, an electromagnetic interference filter is applied to remove significant spike-type interference. Next, inherent DC bias is removed from the in-phase and quadrature data components by applying a dedicated algorithm. The conditioned time series are then passed to the radial-by-radial noise estimation algorithm (Ivic and Torres 2010 and 2011) to obtain a reliable noise power estimate at a given beam position. To maximize the signal-to-noise ratio (SNR), a matched filter is applied to the time series. The matched filter produces a new set of time series with 240 m range resolution (as opposed to the 60 m resolution of the non-filtered time series).

To avoid erroneous detection of ground clutter as newly formed weather phenomena, the matched filtered data is treated next to remove this unwanted presence. In ADAPTS II, the surveillance mode utilized a spatial database of ground clutter powers removed during previous weather scans (Torres et al. 2011, 2012). This database, initially produced by the first (full) weather scan, is continuously updated with data collected at

active beam positions in the weather scan. In the surveillance mode, the clutter power from the database is subtracted from total power estimates at each range gate to produce an approximate weather-signal power. Because ADAPTS II relied on feedback of ground power from previous scans, the weather and surveillance scans were fixed to the same angular positions (i.e. same azimuth and elevation). In ADAPTS III, a new ground clutter filter was introduced which eliminated the need for the ground-clutter-power database allowing independent scanning strategies for weather and detection. Specifics of this filter are presented later in section 2.2. After applying this filter to the matched filtered time series, a power is computed at every position in range.

In the next step, range gates containing strong point clutter are detected and powers, at these gates, are replaced by linear interpolation in range. Then, an array of signal powers is created by subtracting the noise power from powers at each range gate. These signal powers are converted to dB scale and a running average filter (default length of 5) is applied in range to reduce the variance of power estimates. These powers are then used to create a censoring array based on SNR threshold (typical value is 2 dB).

An array of reflectivity estimates is then computed based on signal powers in dB scale; range, atmospheric, and beam steering losses; and radar calibration. Along with the censoring array, reflectivity estimates are used to determine if significant returns (which meet the required continuity and coverage criteria) are present that may warrant setting the corresponding beam position status as active. These active flags from the detection mode are used to update the current weather scanning strategy (see Priegnitz and Heinselman 2013).

2.2. *Ground Clutter Filter Description*

The decision to increase update times by decreasing dwell times is juxtaposed by the need to adequately mitigate ground clutter. For small sample sizes, filtering ground clutter signals from weather signals is nearly impossible. Typical ground clutter filters (i.e., two-, three-, and four-pulse filters) designed to operate with small sample sizes and recover some weather signal, operate in the time domain (see Skolnik 2001 ch. 3 for a review of n-pulse canceler filters). These filters react undesirably to changes in pulse-repetition-time (PRT) by increasing (decreasing) the stopband of the filter with a corresponding decrease (increase) in the PRT. A more significant detriment to the use of these filters is that they cause significant biases in weather signals, even for weather with velocities well away from zero, in order to achieve ground clutter suppression levels needed in an operational environment.

A new filter was designed for the detection processing mode of ADAPTS III. Specifically, the filter is designed to provide unbiased power output in the passband (most of weather and no ground clutter); while, providing a significant signal rejection in the stopband (i.e., ground clutter and weather with narrow spectrum width and zero velocity). The filter design incorporates a velocity-invariant stopband and provides clutter protection for clutter-to-noise ratios (CNR) of up to ~53 dB while operating on small sample sizes of time series data. The filter operates on the pulse-to-pulse phase shift of the signal. With an adjustable notch width (default ±1.5 m/s) and adjustable instantaneous velocity notch depth (default of -60 dB), an ideal notch is created. Pulses that have phase shifts that fall within the filter's notch are scaled to provide ~53 dB of ground clutter suppression (obtained using a Gaussian model with 0.3 m/s spectrum width and 0 m/s velocity), and pulses that have phase shifts that fall outside the filter notch are passed unmodified.

For comparisons, Fig. 1 shows the instantaneous velocity response for the two- (blue line), three- (blue dash), and four-pulse (blue dot-dash) canceler filters and the new moving target indication (MTI) filter driven by signals having PRTs of either 3.0 ms or 0.8 ms with corresponding Nyquist velocities of 7.8 m/s (green line) or 29.3 m/s (green dashes), respectively. The plots show the amount of signal suppression (y-axis in dB) that a sinusoidal signal with a normalized velocity (v/Va) from -1 to 1 would experience if subjected to the filter. It can be seen that the instantaneous velocity response of the filters at 0 is infinitely negative (maximum signal rejection) for the two-, three-, and four-pulse filters and 60 dB for the MTI filter regardless of the PRT. As the instantaneous frequency increases, the filter attenuation reduces toward 0 dB (no signal rejection) for the two-, three-, and four-pulse filters. The normalized velocity response for these filters does not change when the PRT changes which means that the notch width of the filter changes as a function of the PRT. On the other hand, the MTI filter maintains signal rejection at -60 dB (default of the filter) until the passband velocity of 1.5 m/s (default for the filter) is reached (i.e.: v/Va = 1.5/7.8 ≈ 0.19 for the 3-ms PRT and v/Va = 1.5/29.3 ≈ 0.05 for the 0.8-ms PRT). In the passband of the MTI filter the signal is not attenuated (i.e.: 0 dB of rejection).

The instantaneous velocity response does not fully capture how signals from distributed scatterers (such as weather or ground clutter) would be affected by the filters. A standard model for weather and ground clutter is the Gaussian model; thus, with a spectrum width and velocity input, most weather and ground clutter can be adequately modeled. In Fig. 2, the filter gain (dB) (y-axis) is plotted as a function of the normalized mean velocity (v/Va) of each signal (x-axis) for a PRT of 3.0 ms (Va = 7.8 m/s). Gaussian spectrum signals with 0.3 (red line), 0.5 (magenta line), 1.0 (aqua line), 2.0 (green line), and 4.0 m/s (blue line) spectrum widths and different mean velocities spanning -Va to Va are subjected to each filter: three-pulse canceler (top), four-pulse canceler (middle), and MTI filter (bottom). For each mean velocity, the filter gain provides an indication of signal bias and/or rejection. The three- and four-pulse cancelers have good clutter rejection (0.3 m/s spectrum width with 0 m/s velocity) of -43.7 and –61.3 dB, respectively; however, the filters induce significant signal bias at all velocities throughout the Nyquist co-interval. On the other hand, the MTI filter is tuned to

reject narrow spectrum, zero-velocity signals as seen in the filter gain of -53.4 dB for a 0.3 m/s spectrum width signal with 0 m/s velocity. As the width of the signal increases, the filter gain increases toward 0 dB (no attenuation). Additionally, as the signal mean velocity moves away from zero, the filter response rapidly returns to 0 dB gain. The MTI filter induces virtually no bias in the passband and has a much narrower stopband than do the three- or four-pulse cancelers. Table 1, tabulates the filter gain of the three-pulse canceler, four-pulse canceler, and the MTI filter for 0.3, 0.5, 1.0, 3.0, and 4.0 m/s spectrum widths for each velocity of 0 m/s, ±3.4 m/s (i.e. plus/minus half the Nyquist velocity), and ±7.8 m/s (plus/minus the Nyquist velocity). As can be seen in Fig. 3 and table 2 for a PRT of 0.8 ms, the MTI filter has similar characteristics regardless of the PRT; whereas, the three- and four-pulse cancelers exhibit more attenuation in the passband for the short PRT, creating more biases at higher velocities.

An example of the filter performance is seen in the plan-position-indicator (PPI) displays of unfiltered velocity and MTI filtered velocity in Fig. 4a and 4b, respectively. Note that the area near the radar is heavily contaminated with ground clutter (e.g., 0 m/s velocity values near radar) in Fig. 4a. After the application of the MTI filter, the ground clutter contamination is removed. The MTI filter does remove some near-zero velocity, narrow spectrum width weather signals, but most of the weather signals are left unbiased.

3. APPLICATION

On May 19, 2013, the NWRT PAR monitored a dry line as it initiated a severe outbreak of storms and produced several tornados in central Oklahoma. Figure 5 shows three screen captures for consecutive times (19:32:44, 19:32:53, and 19:33:02 CDT) of the ADAPTS GUI early in the event. At 14:32:44 CDT, the ADAPTS GUI (Fig. 5a.) displays circles (indicating azimuth and elevation) of the beam position (relative to antenna boresight) for the current weather scan. The color code at the bottom of the GUI shows that only significant weather (dark green) and neighborhood rules (light green) are active (i.e.: radar is transmitted in these beam position) at this time. The white indicates that no transmission occurred in these beam positions (i.e.: no wasted time at low-interest beam positions). The 90-degree wedge on the compass indicates the antenna boresight was pointing West-Northwest.

Approximately 9 seconds later in Fig. 5b., the ADAPTS GUI indicates that the detection scan detected significant weather (blue filled circles) for additional positions of the weather scanning strategy. Note that the detection beams are not displayed in the ADAPTS GUI; rather, the weather beams are mapped to the closest detection beam for activation such that a single detection beam can activate multiple weather beams. In this case 5 distinct storms initiated both aloft (2.5 to 5 degrees in elevation at several azimuths from -2 to 25 degrees relative to antenna boresight) and at the surface (0.5 degrees in elevation) at approximately -40 degrees azimuth and were isolated from the original storm. Although not shown, these storms were ~75 nm apart from the original storm shown in Fig. 5a.

In another 9 seconds in Fig. 5c., the ADAPTS GUI indicates that new significant and neighborhood rules are actively tracking the newly developed storm.

4. SUMMARY

Evolution of the ADAPTS algorithm has provided a few design challenges. By creating a completely autonomous detection mode in ADAPTS III, flexibility in scheduling multiple scanning strategies can be realized. In this paper, the design considerations for the detection mode were reviewed. To achieve a fast coverage of a large volume of space, small dwell times are needed. This in turn required design considerations to mitigate ground clutter and ultimately a decision to risk loss of narrow-spectra weather signals along the zero-isodop in the detection process. However, the zero-isodop loss is already handled adequately by existing neighborhood rules in the ADAPTS algorithm. The eventual goal of the upgrade was to achieve fast adaptive weather scanning thereby providing meteorologists with faster updates. In section 3, we showed a case where the newly designed detection scan allowed observation of isolated storm initiation while maintaining fast update rates on mature storms. Further evaluations are ongoing which may stem further refinements of the ADAPTS algorithm.

5. ACKNOWLEDGEMENTS

This conference paper was prepared by David Warde, Igor Ivic, and Eddie Forren with funding provided by NOAA/Office of Oceanic and Atmospheric Research under NOAA-University of Oklahoma Cooperative Agreement #NA11OAR4320072, U.S. Department of Commerce. The statements, findings, conclusions, and recommendations are those of the author(s) and do not necessarily reflect the views of NOAA or the U.S. Department of Commerce. We extend a special thanks to members of the MPAR Software Upgrade Project team for their contributions to the research, software design and implementation.

6. REFEERENCES

Heinselman, P. L., S. Torres, R. Adams, C. D. Curtis, E. Forren, I. R. Ivic, D. Priegnitz, J. Thompson, and D. A. Warde, 2009: Phased Array Radar Innovative Sensing Experiment, Preprints, 34th Conference on Radar Meteorology, Williamsburg, VA, Amer. Meteor. Soc., P6.5A

Heinselman, P., S. Torres, D. Russell, R. Adams, 2012: ADAPTS Performance: Can We Further Reduce Update Time?. Preprints, 28th Conf. on Interactive Information and Processing Systems (IIPS) for Meteorology, Oceanography, and Hydrology, New Orleans, LA, USA, Amer. Meteor. Soc., CD-ROM, 6B.4.

Ivic, I., S. Torres, 2010: Online estimation of noise power for weather radars. Preprints, 6th European Conf. on Radar in Meteorology and Hydrology: Adv. in Radar Technology, Sibiu, Romania, National Meteorological Administration, Romania, 30–36.

Ivic, I. R., S. M. Torres, 2011: Online Estimation of Noise Power for Weather Radars. Extended Abstracts, 27th Conference on Interactive Information and Processing Systems (IIPS), Seattle, WA, USA, NSSL/CIMMS, 369.

Priegnitz, D., P. L. Heinselman, S. M. Torres, and R. Adams, 2009: Improvements to the National Weather Radar Testbed Radar Control Interface. Preprints, 34th Conference on Radar Meteorology,
Williamsburg, VA, Amer. Meteor. Soc., P10.10.

Skolnik, M. I., 2001, "Introduction to Radar Systems," 3rd ed., New York, NY: McGraw-Hill.

Torres, S. , C. Curtis, I. Ivic, D. Warde, E. Forren, J. Thompson, R. Adams, D. Priegnitz, 2009: Update on signal processing upgrades for the National Weather Radar Testbed. Preprints, 25th International Conference on Interactive Information and Processing Systems (IIPS) for Meteorology, Oceanography, and Hydrology, Phoenix, AZ, USA, Amer. Meteor. Soc., CD-ROM, 8B.4.

Torres, S. , C. Curtis, I. Ivic, D. Warde, E. Forren, J. Thompson, D. Priegnitz, R. Adams, 2010: Update on signal processing upgrades for the National Weather Radar Testbed. Preprints, 26th International Conference on Interactive Information and Processing Systems (IIPS) for Meteorology, Oceanography, and Hydrology, Atlanta, GA, USA, Amer. Meteor. Soc., CD-ROM, 14B.2.

Torres, S. M., R. Adams, C. Curtis, E. Forren, I. Ivic, D. Priegnitz, J. Thompson, D. Warde, 2011: Software and signal processing upgrades for the National Weather Radar Testbed phased-array radar. Extended Abstracts, 27th Conference on Interactive Information and Processing Systems (IIPS), Seattle, WA, USA, Amer. Meteor. Soc., 12B.3.

Torres, S. , P. Heinselman, R. Adams, C. Curtis, E. Forren, I. Ivic, D. Priegnitz, J. Thompson, D. Warde, 2012: ADAPTS Implementation: Can we exploit phased-array radar's electronic beam steering capabilities to reduce update times?. Extended Abstracts, 28th Conf. on Interactive Information and Processing Systems (IIPS) for Meteorology, Oceanography, and Hydrology, New Orleans, LA, USA, Amer. Meteor. Soc., 6B.3.

FIGURES AND TABLES

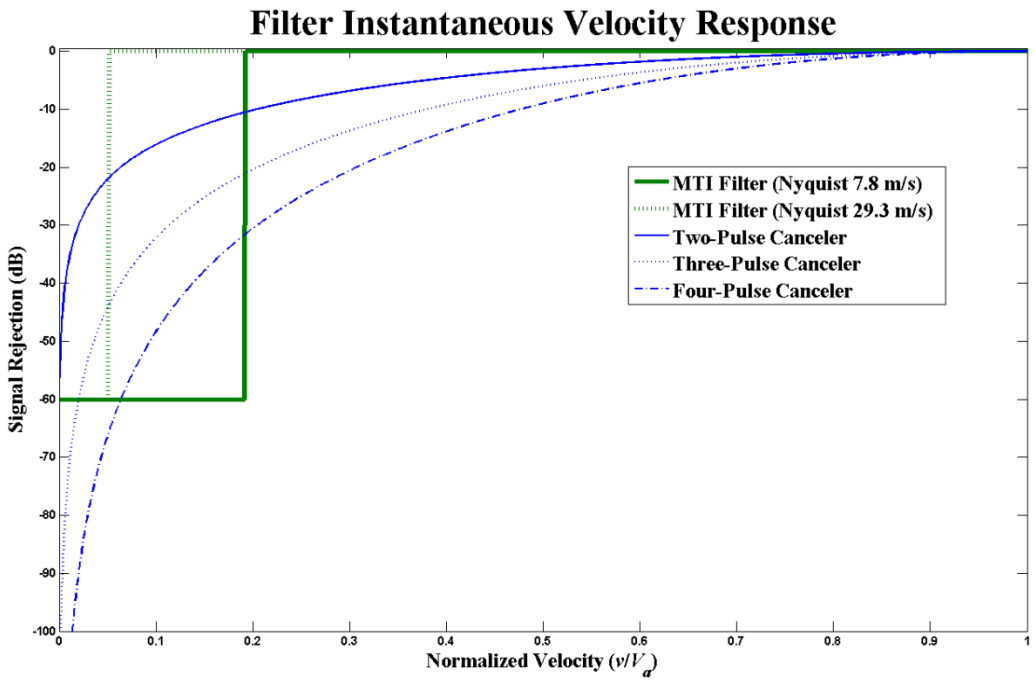

Fig. 1: Plots of signal rejection (dB) (y-axis) as a function of positive normalized velocities (v/V_a) (x-axis) for several filters. The MTI filter with a Nyquist velocity of 7.8 m/s (green line) and 29.3 m/s (green dotted line) have notch widths of ~0.19 and ~0.05 (i.e., 1.5 m/s/Nyquist) that change to maintain an invariant velocity response with PRT changes; whereas, the two- (blue line), three- (blue dotted line), and four-pulse (blue dot-dash line) cancelers have invariant normalized velocity responses causing different velocity responses dependent on PRT changes.

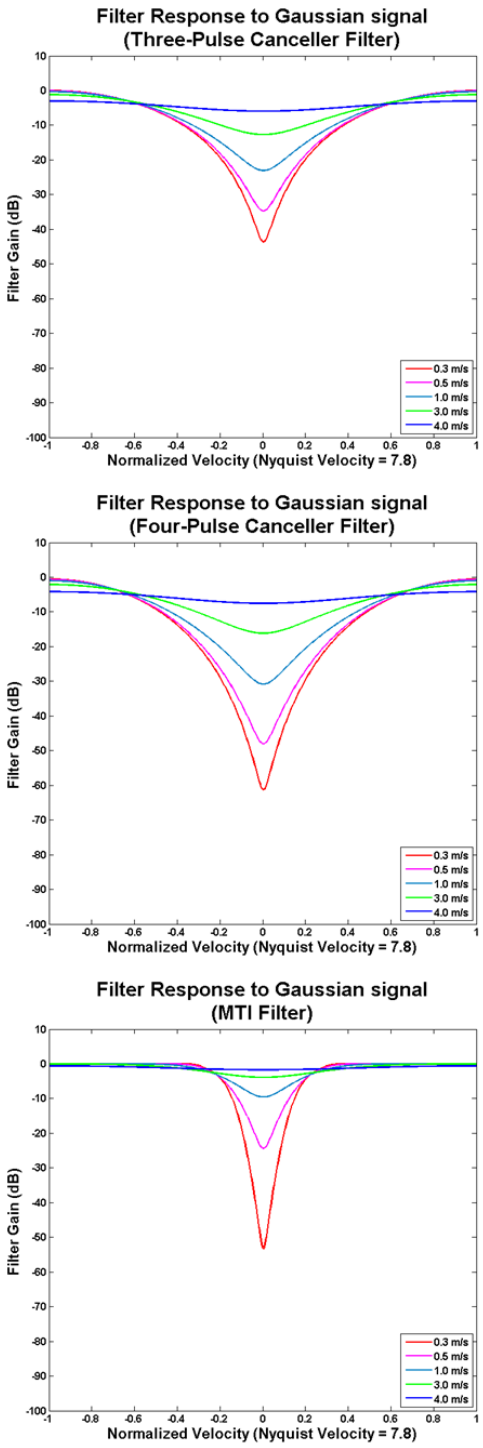

Fig. 2: Filter gain (dB) (y-axis) as a function of the normalized velocity (v/V_a) (x-axis) shown for a PRT of 3.0 ms giving a Nyquist velocity of 7.8 m/s. Gaussian-spectrum signals with 0.3 (red line), 0.5 (magenta line), 1.0 (aqua line), 2.0 (green line), and 4.0 m/s (blue line) spectrum widths and different velocities that span the Nyquist co-interval (i.e., $v = -V_a$ to V_a) are subjected to each filter: three-pulse canceler (top), four-pulse canceler (middle), and MTI filter (bottom).

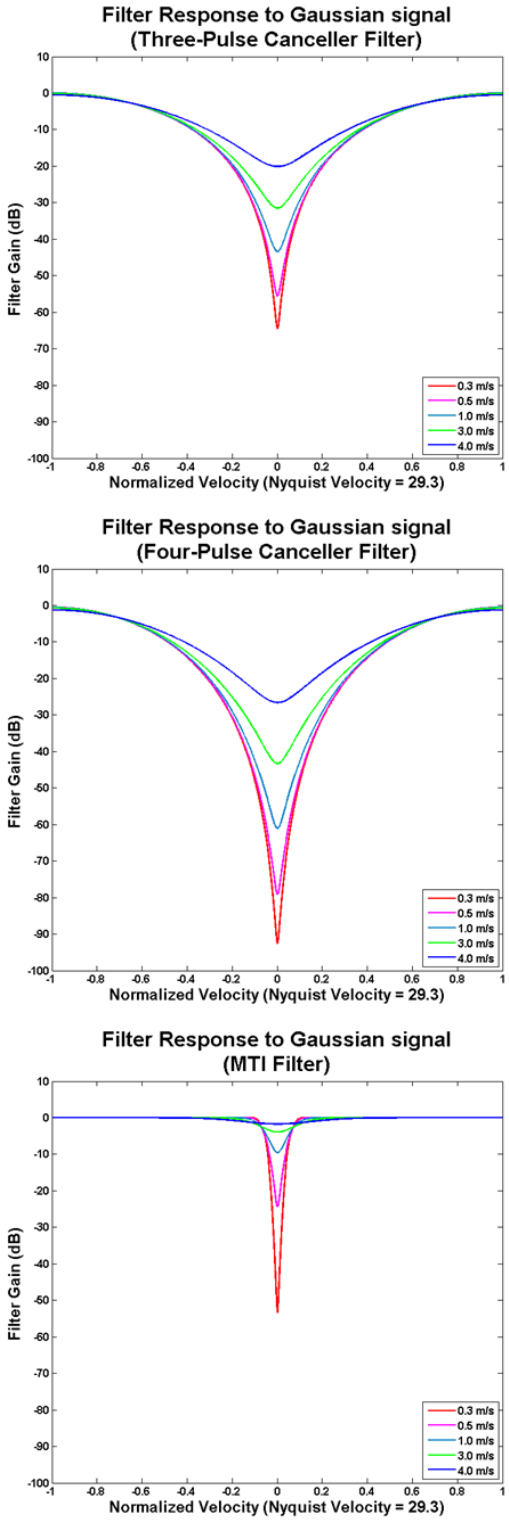

Fig. 3: Same as Fig. 2 except the Nyquist velocity is 29.3 m/s.

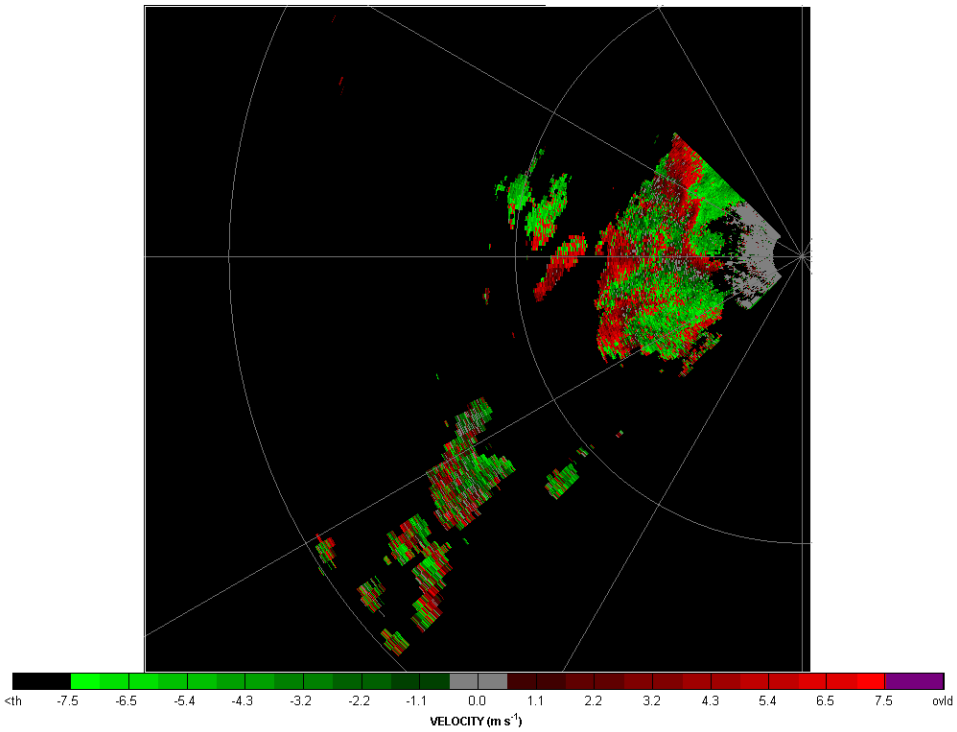

(a)

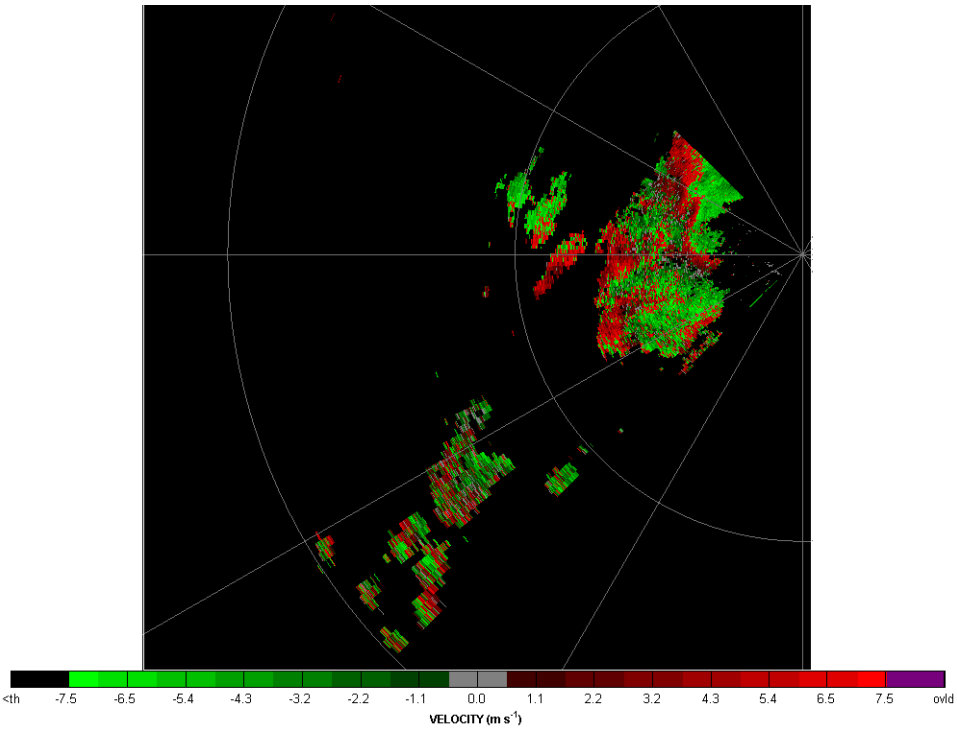

(b)

Fig. 4: PPI of velocity from the NWRT PAR (a) Unfiltered. (b) Filtered using the MTI filter.

Table 1, Filter Gain in dB (V_a = 7.8 m/s)

***v* = 0 m/s**	**Spectrum Width (m/s)**				
Filter	**0.3**	**0.5**	**1.0**	**3.0**	**4.0**
3-Pulse	-43.7	-34.7	-23.0	-12.7	-6.0
4-Pulse	-61.3	-48.0	-30.8	-16.2	-7.5
MTI	-53.2	-24.4	-9.5	-3.9	-1.7
***v* = ± 3.9 m/s**					
3-Pulse	-6.0	-6.0	-5.5	-4.7	-4.3
4-Pulse	-9.5	-9.2	-8.1	-6.3	-5.6
MTI	0.0	0.0	-0.1	-0.7	-1.1
***v* = ± 7.8 m/s**					
3-Pulse	0.0	-0.1	-0.4	-1.2	-3.0
4-Pulse	0.0	-0.7	-1.0	-2.1	-4.2
MTI	0.0	0.0	0.0	0.0	-0.6

Table 2, Filter Gain in dB (V_a = 29.3 m/s)

***v* = 0 m/s**	**Spectrum Width (m/s)**				
Filter	**0.3**	**0.5**	**1.0**	**3.0**	**4.0**
3-Pulse	-64.6	-55.6	-43.4	-31.5	-20.1
4-Pulse	-92.7	-79.1	-61.1	-43.3	-26.6
MTI	-53.4	-24.5	-9.6	-3.9	-1.7
***v* = ± 14.7 m/s**					
3-Pulse	-6	-6	-5.9	-5.8	-5.3
4-Pulse	-9.6	-9.5	-9.4	-8.9	-7.6
MTI	0	0	0	0	0
***v* = ±29.3 m/s**					
3-Pulse	0	0	0	-0.1	-0.5
4-Pulse	-0.5	-0.5	-0.6	-0.7	-1.2
MTI	0	0	0	0	0

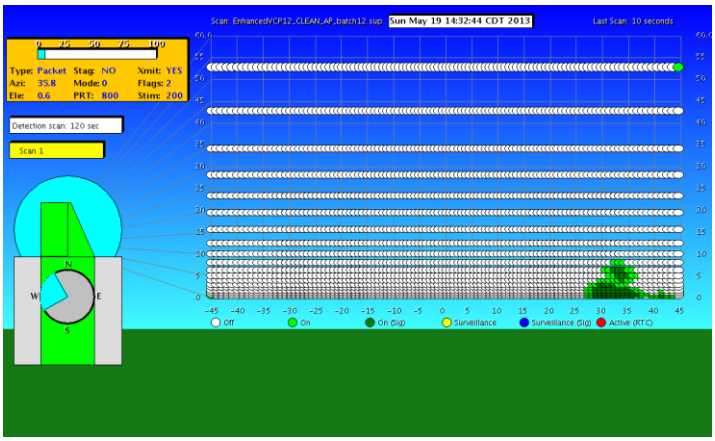

Fig. 5a. NWRT PAR ADAPTS GUI captured on May 19, 2013 at 14:32:44 CDT shows weather scan beams that are activated by significant weather (dark green) or neighborhood rules (light green). The white indicates that no transmission occurred in these beam positions. (Image by David Preignitz)

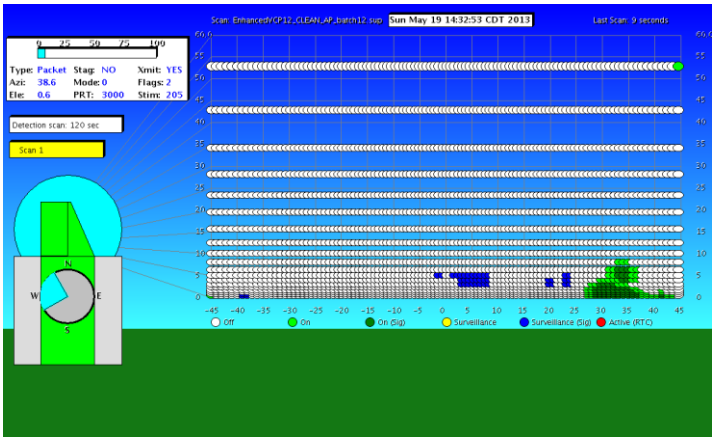

Fig. 5b. NWRT PAR ADAPTS GUI captured on May 19, 2013 at 14:32:53 CDT (9 seconds after Fig 5a) shows weather beams (color scales same as in Fig. 5a.) with weather beams (blue) that were turned on by significant weather detection in the detection mode. Note that the detection beams are not displayed; rather, the weather beams are mapped to the closest detection beam for activation. (Image by David Preignitz)

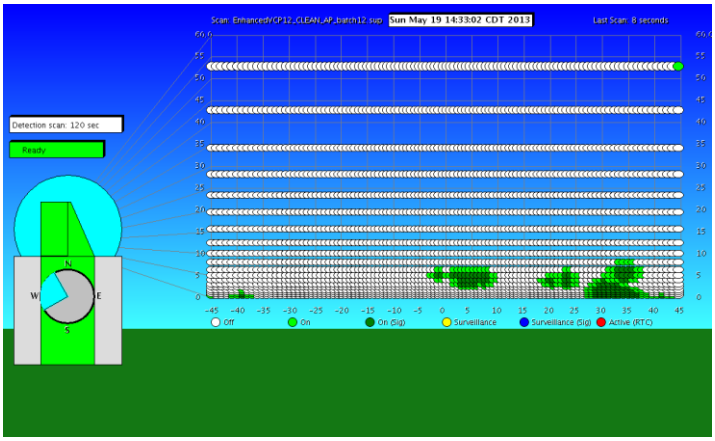

Fig. 5c. NWRT PAR ADAPTS GUI captured on May 19, 2013 at 14:33:02 CDT (18 seconds after Fig 5a) shows weather beams (color scales same as in Fig. 5a.). (Image by David Preignitz)